Biosensors and Bioelectronics xxx (xxxx) xxx

Contents lists available at ScienceDirect

Biosensors and Bioelectronics

journal homepage: http://www.elsevier.com/locate/bios

A test strip platform based on a whole-cell microbial biosensor for simultaneous on-site detection of total inorganic mercury pollutants in cosmetics without the need for predigestion

Mingzhang Guo [a,b,1], Jili Wang [b,1], Ruoxi Du [b], Yanger Liu [b], Jiani Chi [b], Xiaoyun He [a,b], Kunlun Huang [a,b], Yunbo Luo [a,b], Wentao Xu [a,b,*]

[a] Beijing Advanced Innovation Center for Food Nutrition and Human Health, College of Food Science and Nutritional Engineering, China Agricultural University, Beijing, 100083, China

[b] Key Laboratory of Safety Assessment of Genetically Modified Organism (Food Safety), Ministry of Agriculture, Beijing, 100083, China

ARTICLE INFO

Keywords:
Whole cell biosensor
Mercury
Test strip
On-site detection

ABSTRACT:

Mercury pollutants such as mercuric chloride ($HgCl_2$), mercurous chloride (Hg_2Cl_2) and mercuric ammonium chloride ($Hg(NH_2)Cl$) are often found in cosmetics. Previous attempts at the on-site detection of mercury were hindered by the complicated and dangerous pretreatment procedure of converting various forms of mercury to Hg (II) ions. In this study, a test strip platform was developed based on a whole-cell microbial biosensor for the simultaneous detection of soluble and insoluble inorganic mercury pollutants in cosmetics without the need for predigestion. The genetic circuits with constitutively expressed MerR as sensor proteins and inducible red fluorescent protein (RFP) as the reporter were introduced into *Escherichia coli* to construct the mercury detection biosensor. The RFP fluorescence intensity of this biosensor showed a excellent linear relationship ($R^2 = 0.9848$) with the Hg (II) concentration ranging from 50 nM to 10 μM in Luria-Bertani (LB) broth. Further research indicated that this biosensor could respond not only to Hg (II) ions but also to insoluble Hg_2Cl_2 and Hg_2Cl_2. The transcriptomic results confirmed the mercury conversion ability of the whole-cell biosensor from a gene expression perspective. This biosensor was embedded on filter paper to form a test strip, which could be used to determine whether the total inorganic mercury pollutants in cosmetics exceeded 1 mg/kg. Therefore, this strip provided a low cost, easy-to-use, and instrument-independent method for the detection of mercury pollution in cosmetics, while this study revealed the unique advantages of microbial biosensors in the automatic bioconversion of targets.

1. Introduction

In recent decades, mercury pollution has been prevalent in water, food, cosmetics, and even the atmosphere, which poses a serious threat to human health and the social economy (Spiegel, 2017). Mercury pollution can present in different forms, such as elemental mercury (Hg) (Gonzalez-Raymat et al., 2017), $HgCl_2$, Hg_2Cl_2 (Lori et al., 2015), methylmercury (CH_3Hg) (Grandjean et al., 2010) and $Hg(NH_2)Cl$ (Pelclova et al., 2002). These molecules can enter the human body through the diet, the skin, as well as breathing, and accumulate in the vital organs and tissues, causing organ dysfunction and irreversible damage to the nervous system (Bjorklund et al., 2017). Therefore, the World Health Organization (WHO) has prescribed the permitted maximum levels of mercury in different samples to control the hazard posed by mercury.

The development of rapid, simple, and cost-effective methods for the on-site detection will promote the management and remission of heavy metal pollution. Currently used methods, such as atomic absorption spectroscopy, electron capture devices, inductively coupled plasma optical emission, mass spectrometry, as well as some PCR based methods rely on expensive facilities (Leopold et al., 2010; Zhu et al., 2016; Cheng et al., 2016). Some on-site detection platforms have been developed based on gold nanoparticles (Guo et al., 2012; Feng et al., 2018; Shao

* Corresponding author. Laboratory of food safety and molecular biology, College of Food Science and Nutritional Engineering, China Agricultural University, No. 17, Qinghua East Road, Haidian district, Beijing, 100083, China.
E-mail address: xuwentao@cau.edu.cn (W. Xu).

[1] These authors contributed equally to this work.

https://doi.org/10.1016/j.bios.2019.111899
Received 15 September 2019; Received in revised form 5 November 2019; Accepted 14 November 2019
Available online 18 November 2019
0956-5663/

et al., 2019) and functional nucleic acids (Xu et al., 2017; Xiao et al., 2019; Zhu et al., 2019). However, these methods can only sense the soluble metal ions. For some insoluble heavy metal pollutants such as Hg_2Cl_2 and $Hg(NH_2)Cl$, these methods do not produce any response. For the detection of total mercury, predigestion of the sample with a strong oxidative acid is required to convert other forms of mercury to Hg (II) ions (Patel-Sorrentino et al., 2011), which is complex and dangerous to use for on-site detection.

A whole-cell microbial biosensor is a novel device for the qualitative and quantitative detection of molecules (Du et al., 2019; Guo et al., 2019) or processes (such as nanotoxicity, Hondroulis et al., 2010) by microorganism cells. Whole-cell microbial biosensors provide an alternative method for mercury detection. By simulating the mercury resistance systems of bacteria, whole-cell mercury biosensors use merR protein to sense the mercury and transform the concentration of mercury into the expression of the reporter gene (Harkins et al., 2004; Mahbub et al., 2017; Cai et al., 2018). Previous reports showed that whole-cell microbial biosensors exhibit significant advantages such as being inexpensive, simple to operate and prevent interference. This study proposes an additional advantage resulting from the metabolic activity of the microbial cells, namely the "automatic conversion ability" for different forms of mercury. Consequently, whole-cell microbial biosensors possess the potential to provide an on-site mercury detection method without the need of predigestion. What's more, whole-cell microbes have shown numerous integration with test strips (Stocker et al., 2003; Struss et al., 2010; Li et al., 2011), indicating the potential of using cell sensors to develop test strips.

In cosmetics, soluble $HgCl_2$, as well as insoluble Hg_2Cl_2 and $Hg(NH_2)Cl$ are often added for the whitening effect (Chan, 2011; Özkaya et al., 2010). However, if the permitted maximum levels for these mercury compounds are exceeded, it can result in chronic toxicity to the skin and organs. In this study, a microbial biosensor based test strip was developed for the simultaneous on-site detection of soluble and insoluble inorganic mercury pollution in cosmetics without the need for predigestion. Therefore, consumers can use this strip at home to test for the presence of mercury in cosmetics. This test strip could reduce the cost and technical requirement of inorganic mercury detection, and therefore promote the management and remission of mercury pollutants. More importantly, this work showed the great potential of whole cell biosensors in on-site detection of pollution. The complex pretreatment process that previously need to be manually completed now can be conducted by the biosensor cells automatically, which will make the detection process simpler, safer, and more pleasant.

2. Materials and methods

2.1. Chemicals and bacteria

$HgCl_2$ (99.5%) was purchased from Xiya Reagent (Shandong, China). Hg_2Cl_2 (99.5%) and $Hg(NH_2)Cl$ (98%) were purchased from Rhawn Chemical Technology (Shanghai, China). *Escherichia coli* DH5α (laboratory preservation) was used as receptor cells for all the plasmids in this study. Genewiz Inc (Suzhou, China) synthesized the codon-optimized *rfp*, *egfp*, and *merR* genes (Table S1), while Ruibio Biotech (Beijing, China) conducted the oligonucleotide synthesis and plasmid sequencing.

2.2. Construction of the whole-cell mercury biosensor

Endonuclease digestion site-modified pENTR/D-TOPO (Thermo Fisher, Waltham, USA) was used as a plasmid backbone. The *merR* gene with a constitutive promoter was inserted into the plasmid backbone using *Xho*I/*Hind*III restriction enzyme digestion and a T4 ligation reaction. Then *rfp* or *egfp* genes with a merR binding promoter were inserted into the plasmid backbone using *Kpn*I/*Xho*I restriction enzyme digestion and a T4 ligation reaction. The constructed plasmid was transformed into *E. coli* DH5α, cultured in LB broth, and stored with 50% glycerol at −80 °C until used.

2.3. Fluorescence measurement

The biosensors were first activated by overnight growth in LB broth with kanamycin. Before the bioassay, the activated biosensors were diluted into fresh LB broth containing kanamycin and incubated at 37 °C and 220 rpm until OD600 reached approximately 0.6. Then, 5 mL biosensor cultures, 5 mL fresh LB broth with kanamycin, and 100 μL heavy metal ion solution were mixed in 50 mL flasks and incubated at 37 °C and 220 rpm for 2 h. Furthermore, 200 μL cultures were obtained for the measurement of OD600. An additional 2 mL cultures were centrifugated at 10000×*g*, and the sediment was resuspended with 200 mL 0.9% saline. The fluorescence intensity of the resuspended solution was measured using a Cary Eclipse Fluorescence Spectrophotometer (Agilent Technologies, Santa Clara, USA). For RFP, the excitation wavelength was 587 nm, and the emission wavelength was 610 nm. Moreover, 5 mL biosensor cultures, 5 mL fresh LB broth with kanamycin, and 100 μL distilled water were mixed and measured as the background OD and fluorescence intensity. The relative fluorescence intensity (RFI) was calculated using (sample fluorescence intensity/sample OD) – (background fluorescence intensity/background OD).

2.4. Preparation of test strips

The biosensor cells were first activated by overnight growth in LB broth with kanamycin. Before the bioassay, the activated biosensors were diluted into fresh LB broth containing kanamycin and incubated at 37 °C and 220 rpm until the OD600 reached approximately 0.8. Then, 6 mL of the culture was centrifuged and resuspended with 200 μL protectant buffer (0.5% peptone, 0.3% nutrient broth, 10% gelatin, 1% sodium ascorbate, 5% raffinose, and 5% sodium glutamate). The resuspended cells were placed on a filter paper disc with a diameter of 25 mm, air-dried, and stored at 4 °C until use.

2.5. Detection procedures

For the detection of mercury pollution in cosmetics, ultra-pure water was added to a 1 g sample to reach a total volume of 5 mL. After thorough mixing, 200 μL was placed onto the test paper and incubated at 37 °C for 6 h. Whether the total mercury pollution in cosmetics exceeded 1 mg/kg, depended on whether or not the test paper turned red.

2.6. Transcriptomic analysis

A total amount of 3 μg RNA per sample was used as input material for the RNA sample preparations. Sequencing libraries were generated using a NEBNext® Ultra™ Directional RNA Library Prep Kit for Illumina (NEB, USA) following the recommendations of the manufacturer, while index codes were added to attribute sequences to each sample. After adenylation of the 3' ends of the DNA fragments, a NEBNext Adaptor with a hairpin loop structure was ligated to prepare for hybridization. The library fragments were purified with an AMPure XP system (Beckman Coulter, Beverly, USA) to select cDNA fragments of preferentially 150–200 bp in length. PCR was performed with Phusion High-Fidelity DNA polymerase, Universal PCR primers, and an Index (X) Primer. The library preparations were sequenced on an Illumina Hiseq platform, and paired-end reads were generated.

2.7. Bioinformatics and statistics analysis

Raw data from the FASTQ format were processed via in-house Perl scripts. Clean data were obtained by removing reads containing adapters and ploy-N, as well as low-quality reads from raw data. The clean reads were aligned to reference the genome using Bowtie2-2.2.3 (Langmead et al., 2009). HTSeq v0.6.1 (Anders et al., 2015) was used to count the

read numbers mapped to each gene. Then, Fragments Per Kilobase of transcript sequence per Million base pairs sequenced (FPKM) of each gene was calculated based on the length of the gene, while read count was mapped to this gene. Differential expression analysis of two groups was performed using the DESeq R package (1.18.0) (Anders and Huber, 2010). The resulting P-values were adjusted using the Benjamini and Hochberg's approach for controlling the false discovery rate. Genes with an adjusted P-value <0.05 found by DESeq were assigned as differentially expressed. KOBAS software (Mao et al., 2005) was used to test the statistical enrichment of differentially expressed genes in the KEGG pathways.

Each determination was repeated three times, and all values were expressed as the arithmetic mean ± standard deviation (SD). The data were analyzed using a one-way analysis of variance (ANOVA) followed by a *t*-test.

3. Results and discussion

3.1. Construction and assessment of the whole-cell mercury biosensor cMerR-RFP

Traditional whole-cell mercury biosensors used the *merR* gene and its native promoter, which formed feedback regulation at the intracellular MerR protein level. In this study, the biosensor cMerR-RFP was constructed using a constitutive P479 as the promoter of the sensor protein (Fig. S1). The relative constant expression level of MerR might achieve an enhanced linear response to mercury via the biosensor. Biosensor cMerR-RFP was incubated with different mercury ion concentrations in LB broth to assess its detection ability. As shown in Fig. 1A, the RFP fluorescence intensity exhibited excellent linear correlation with the Hg (II) ion concentration in a range of 50 nM to 10 μM. Although the detection limit of biosensor cMerR-RFP was similar to that of the previously reported MerR biosensors, the linear correlation ($R^2 = 0.9848$) of the biosensor in this study was much better than previous ones (Mahbub et al., 2017). Mercury concentrations exceeding 10 μM induced the severe toxicity of the biosensor cells, inhibiting their growth (Fig. S2). Observation with a fluorescence microscope produced the visual images of RFP in the cMerR-RFP cells in the presence of Hg (II) (Fig. 1B). The specificity of biosensor cMerR-RFP was then validated in LB broth. Fig. 1C indicates that the biosensor displayed no or an extremely low response to other metal ions such as Pb (II), Zn (II), Fe (II), Cd (II), Co (II), Ag (I), Cu (I) and Ni (I) at their respective 10 μM concentrations.

3.2. Biosensor cMerR-RFP can sense different forms of mercury

Mercury compounds in cosmetics primarily include $HgCl_2$, Hg_2Cl_2, and $Hg(NH_2)Cl$. Therefore, a biosensor that could simultaneously detect all three compounds would be an ideal mercury detection method for cosmetic samples. To determine whether biosensor cMerR-RFP could respond to Hg_2Cl_2 and $Hg(NH_2)Cl$, the biosensor was incubated with these compounds in LB broth. After 2 h of incubation, Hg_2Cl_2, and $Hg(NH_2)Cl$, could also induce the RFP expression of biosensor cMerR-RFP (Figs. 1C and 2A). However, organic mercury compound CH3Hg could not induce the RFP expression of biosensor cMerR-RFP. Since Hg_2Cl_2 and $Hg(NH_2)Cl$ are insoluble in water, and Hg(II) represented the

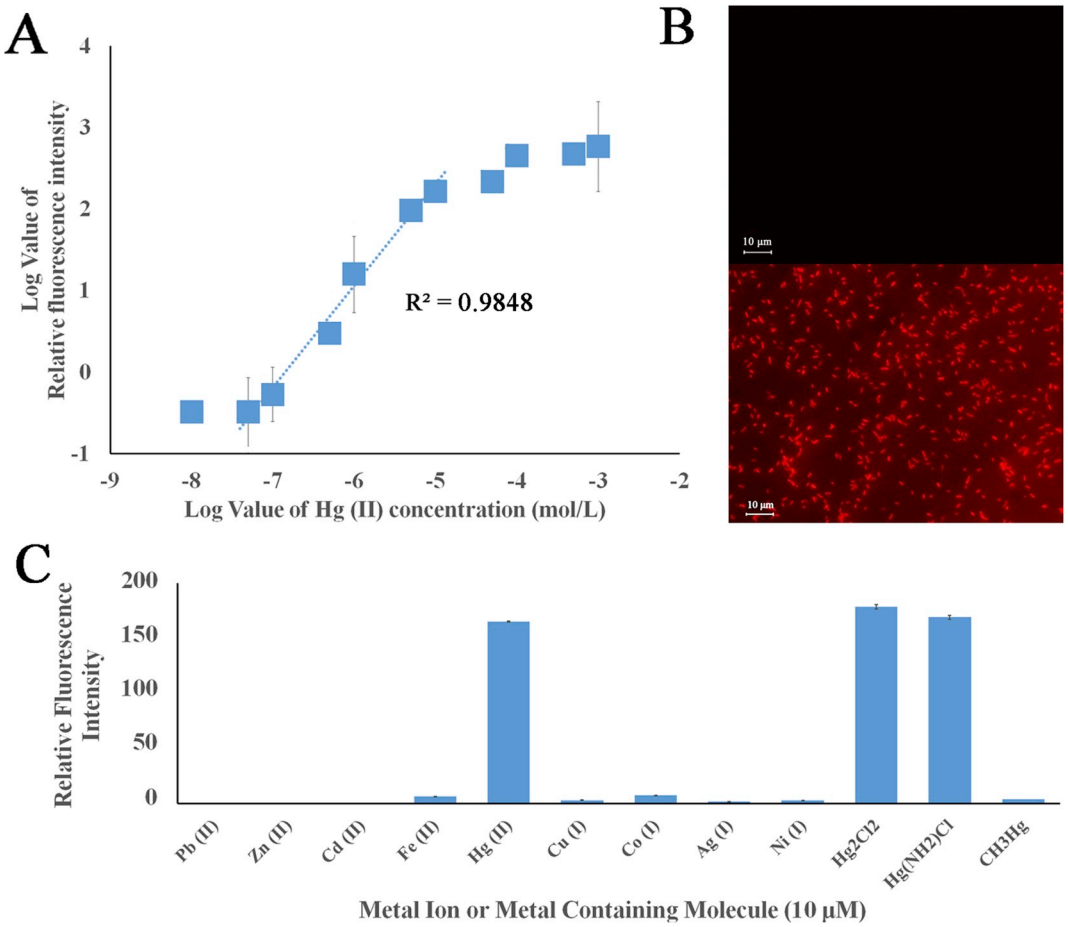

Fig. 1. The response of biosensor cMerR-RFP to mercury and other ions in the LB broth. (A) The linear relationship between the RFP fluorescence intensity of the biosensor and the Hg (II) ion concentration. (B) Observation of the biosensor cMerR-RFP without Hg (II) (upper), and with 10 μM Hg (II) (lower) using a fluorescence microscope. (C) The response of biosensor cMerR-RFP to 10 μM of various metal ions, and different forms of mercury.

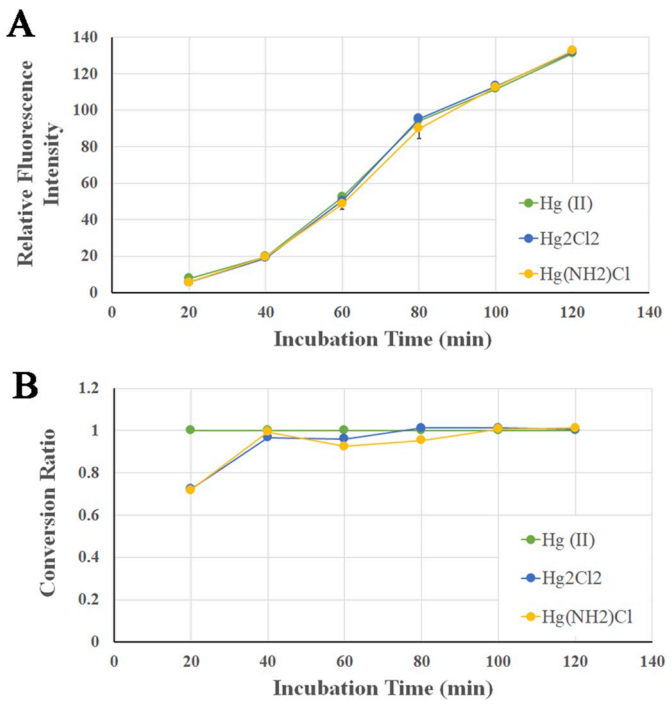

Fig. 2. Relative Fluorescence Intensity (RFI) (A) and Conversion Ratio (B) of biosensor cMer-RFP after incubation with $HgCI_2$, Hg_2Cl_2, and $Hg(NH_2)Cl$. The Conversion Ratio was calculated using the RFI of biosensor incubated with Hg_2Cl_2 or $Hg(NH_2)Cl$ divided by the RFI of the biosensor incubated with Hg (II).

mercury form binding with the MerR protein, it could be conjectured that biosensor cMerR-RFP could convert Hg_2Cl_2 and $Hg(NH_2)Cl$ to soluble Hg (II). The Conversion Ratio could be revealed by the RFI of the biosensor incubated with Hg_2Cl_2 or $Hg(NH_2)Cl$ divided by the RFI of the biosensor incubated with Hg (II). Fig. 2B shows that the conversion process from Hg_2Cl_2 to Hg (II), as well as from $Hg(NH_2)Cl$ to Hg (II) could be completed in 40 min in LB broth, with the final conversion rate exceeding 92%.

3.3. Transcriptomic analysis of the insoluble mercury conversion ability of biosensor cMer-RFP

Transcriptomic analysis was used to explore the uptake mechanism and conversion of insoluble mercury by biosensor cMer-RFP. High throughput sequencing of the transcriptome of biosensor cMer-RFP incubated with $HgCl_2$ (R2 group, including R21 and R22), Hg_2Cl_2 (R1 group, including R11 and R12), $Hg(NH_2)Cl$ (RN group, including RN1 and RN2), and Hg-free water (control group, EC1 and EC2) generated 14.252 ± 3.017 million clean reads per sample on average. The FPKM of each gene was calculated to assess the expression level of the gene, which could eliminate the influence of sequencing depth and gene length. The heatmap of FPKM (Fig. 3A) showed the gene expression profile of each sample. According to the sample clustering in this heatmap, biosensor cMer-RFP incubated with $HgCl_2$, Hg_2Cl_2, and $Hg(NH_2)Cl$ showed similar gene expression profiles, which were distinctly different from the control group. This result indicated that insoluble Hg_2Cl_2 and $Hg(NH_2)Cl$ have a similar influence on the metabolism of biosensor cells with soluble $HgCl_2$ while providing transcriptomic evidence for the conjecture that Hg_2Cl_2 and $Hg(NH_2)Cl$ were converted to Hg(II) in the cells. Differential expression analysis was conducted between the R1 group and the R2 group, as well as between the RN group and the R2 group to determine the mechanism of this conversion process. The results revealed 129 up-regulated gene expressions and 111 down-regulated gene expressions in the R1 group, and 181 up-regulated gene expressions and 215 down-regulated gene expressions in the RN group (Fig. S3). KEGG pathway analysis of these differentially expressed genes showed that "Biosynthesis of Siderophore Group Nonribosomal Peptides" was the most affected pathway in both the R1 group and the RN group when compared with the R2 group (Fig. 3B). There are seven genes in the pathway "Biosynthesis of Siderophore Group Nonribosomal Peptides" of *Escherichia coli*. The expression of five genes belonging to this pathway was significantly inhibited when incubated with Hg_2Cl_2 and $Hg(NH_2)Cl$ (Fig. 3C). The production of "Biosynthesis of Siderophore Group Nonribosomal Peptides" included nonribosomal peptides enterochelin, which can assist bacteria in absorbing iron from insoluble iron compounds (Chen et al., 2014). Therefore, it is reasonable to speculate that enterochelin, its derivatives or its analogs might promote the uptake of mercury from insoluble Hg_2Cl_2 and $Hg(NH_2)Cl$ (Fig. 3D), while the inhibition of these gene expressions might signify the resistance mechanism of biosensor cells to reduce the uptake of mercury. However, the specific enzyme functionality involved in the conversion of Hg_2Cl_2 and $Hg(NH_2)Cl$ to Hg(II) remains unknown.

3.4. The biosensor cMer-RFP-based test strip exhibited a specific response to mercury-containing molecules

Due to its portability and flexibility, employing a test strip for the on-site detection of mercury is preferable to a microbial biosensor in LB broth. The protectants were used to shield the biosensor cells from desiccation stress while fixing them on the filter paper discs. When the fluorescent proteins reached a certain concentration, they displayed a visible color on filter paper. Green fluorescent protein (GFP) and RFP were the most commonly used fluorescent proteins. Therefore, biosensor cMerR-RFP and cMerR-GFP were constructed, and the visual effects of these two fluorescent proteins on the test strip were compared. Fig. 4A illustrates that the color of RFP was more distinguishable from the control filter paper discs than GFP, subsequently leading to biosensor cMerR-RFP being used in the test strip. Sensitivity analysis showed that part of the test strip incubated with 1 μM or 2.5 μM Hg (II) turned red. Furthermore, when the concentration of Hg (II) reached 5 μM, the entire test strip exhibited a visible red color (Fig. 4B), indicating that the sensitivity of the test strip was 1 μM of Hg (II).

Inorganic mercury components, such as $HgCl_2$, Hg_2Cl_2, and $Hg(NH_2)Cl$, are often added into cosmetics for the whitening effects. Organic mercury, which has no whitening effects and high toxicity, usually does not appear in cosmetics. To test whether the biosensor based test strip could simultaneously detect different forms of inorganic mercury, 10 μM of $HgCl_2$, 5 μM Hg_2Cl_2 and 10 μM $Hg(NH_2)Cl$ were added to the test strip, respectively. Fig. S4 indicates that the test strip ultimately exhibited a similar color, provided that the molar number of Hg were the same, regardless of which form of mercury was present. This results revealed that the biosensor cells on the test strip could also achieve the conversion of Hg_2Cl_2 and $Hg(NH_2)Cl$ to Hg (II), and then induce the expression of the RFP. The test strip incubated with 10 μM $HgCl_2$ showed a visible red color within 3 h, while the test strip incubated with 5 μM Hg_2Cl_2 and 10 μM $Hg(NH_2)Cl$ also turned red within 3 h. Therefore, the conversion from Hg_2Cl_2 and $Hg(NH_2)Cl$ to soluble Hg (II) on the test strip could be completed by the biosensor cells in no more than 3 h, and this process did not influence the detection results. The total incubation time was set as 6 h to make the results more distinguishable. Traditional mercury detection methods need the procedure of predigestion, which will take at least 5 h. Thus the total detection time of this test strip and traditional methods is similar. On other counts, this test strip is safe and needs no instrument, which makes it more convenient for on-site detection of mercury than traditional methods.

3.5. Using the cMer-RFP-based test strip to detect total inorganic mercury pollutants in cosmetics

In most countries, the permitted maximum level of mercury in cosmetics is 1 mg/kg. Therefore, the 1 g sample was suspended in ultra-pure

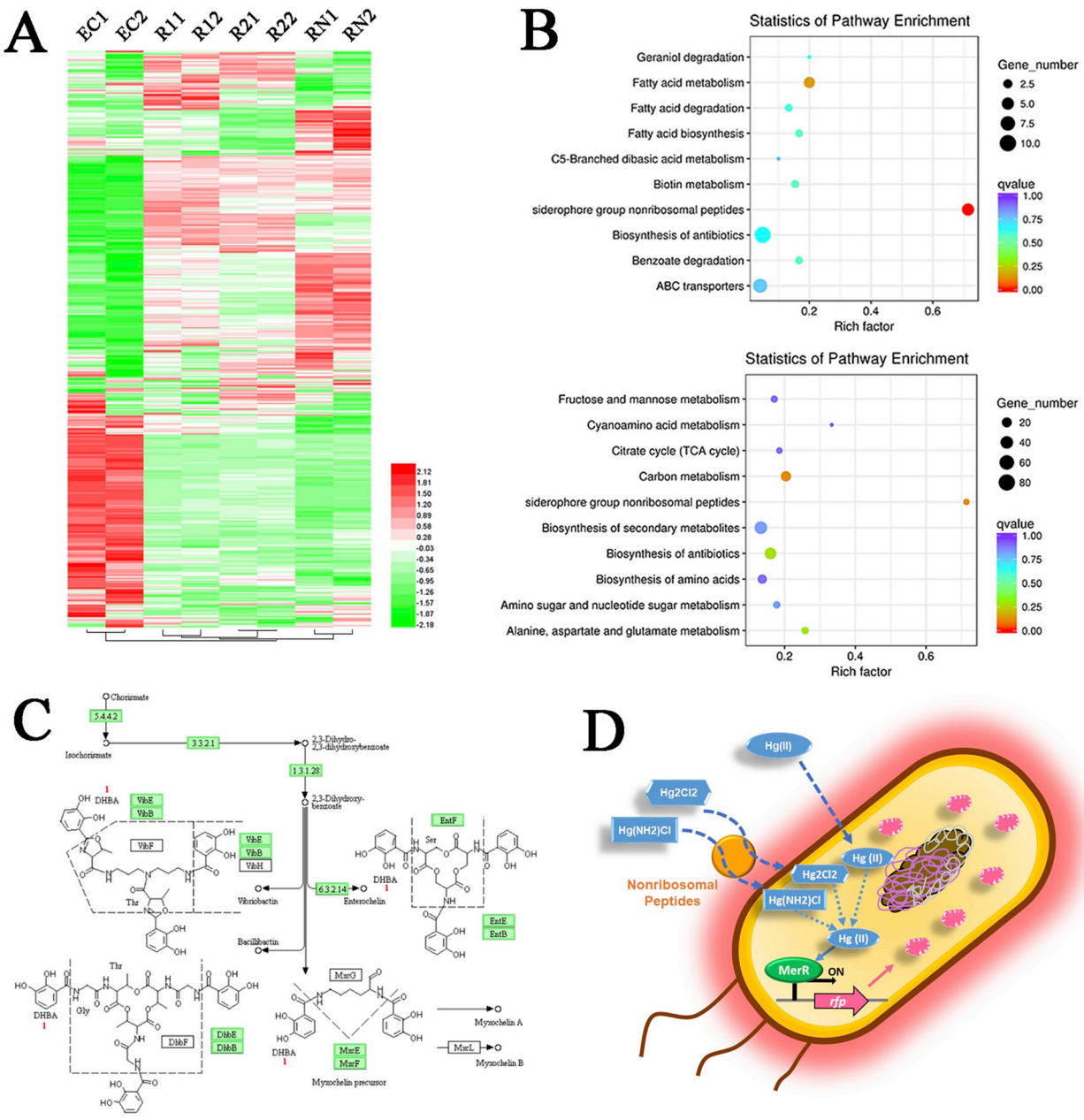

Fig. 3. Potential mechanism of cMer-RFP cells to detect insoluble mercury components revealed by transcriptomics. (A) Gene expression heatmap of different samples according to the FPKM of each gene. (B) KEGG pathway enrichment analysis of differentially expressed genes when comparing the R1 group with the R2 group (Upper), and comparing the RN group with the R2 group. (C) Partial metabolic pathway of "Biosynthesis of siderophore group nonribosomal peptides." (D) Sketch map of the potential mechanism of cMer-RFP cells to detect insoluble mercury components.

water with a total volume of 5 mL to reach a limited value of about 1 μM, which was also the threshold concentration for the test strip to turn red. The entire detection process is quite simple (Fig. 5), and no specific instrument is required. To confirm whether the test strip would work well with the components in cosmetics during the detection process, 0.1 mg/kg, 1 mg/kg, and 10 mg/kg of mercury representing $HgCl_2$, Hg_2Cl_2, and $Hg(NH_2)Cl$, were respectively added to a commercial whitening essence. Then, the samples were detected using the test strip according to the process in Fig. 5A. Fig. 5B shows that regardless of mercury type, the test strips incubated with samples containing 0.1 mg/kg mercury failed to turn red, while the test strips incubated with samples containing 1 mg/kg mercury turned partly red and the test strips incubated with samples containing 10 mg/kg mercury turned entirely red. These results indicated that this test strip possessed the stability to resist the interference of the complex ingredients in cosmetics. Furthermore, three forms of mercury were mixed in equal and different proportions (Fig. 5C, Table S2) and added to the commercial whitening essence. The test strip could successfully distinguish whether the concentration of total inorganic mercury in the samples exceeded 1 mg/kg.

4. Conclusion

In conclusion, a microbial biosensor-based test strip is developed for the qualitative detection of both soluble and insoluble mercury pollution in cosmetics. Since the cells in this biosensor can automatically convert the insoluble Hg_2Cl_2 and $Hg(NH_2)Cl$ to soluble Hg (II) ions, no predigestion process is required for this test strip. Whether the total mercury pollution in cosmetics exceeded 1 mg/kg, depends on whether the test paper turns red, while no specialized instrument is required during the entire detection process. Therefore, this strip provides a low cost, easy-

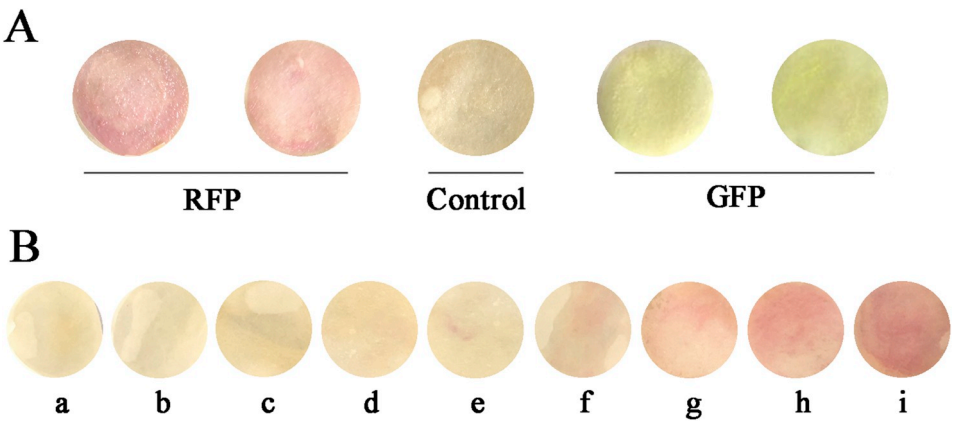

Fig. 4. Construction of the test strip based on the microbial biosensor. (A) Comparison of the visual effect of the GFP and RFP on the test strip. (B) Sensitivity analysis of the test strip with different concentrations of Hg (II). (a)–(i) indicate 0 μM, 0.25 μM, 0.5 μM, 0.75 μM, 1 μM, 2.5 μM, 5 μM, 7.5 μM, and 10 μM Hg (II) respectively.

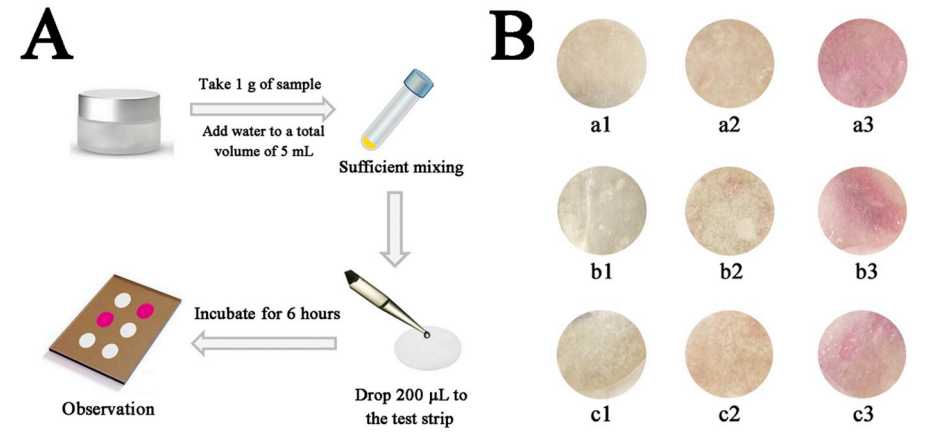

C

$HgCl_2$ (μM)	Hg_2Cl_2 (μM)	$Hg(NH_2)Cl$ (μM)	Total inorganic Hg (μM)	Whether Hg>1 μM	AFS results (μM)	Test Strip Result
0.01	0.01	0.01	0.03	No	0.02 ± 0.00	
0.1	0.1	0.1	0.3	No	0.26 ± 0.02	
1	1	1	3	Yes	2.89 ± 0.05	
10	10	10	30	Yes	27.05 ± 0.24	

Fig. 5. Applying the test strip to detect the total inorganic mercury in cosmetics samples. (A) Detection process (B) Test strips incubated with $HgCl_2$, Hg_2Cl_2, and $Hg(NH_2)Cl$, respectively. a, b, c indicate $HgCl_2$, Hg_2Cl_2, $Hg(NH_2)Cl$; 1, 2, 3 indicate 0.1 mg/kg, 1 mg/kg, and 10 mg/kg of mercury. (C) Test strip results and Atomic Fluorescence Spectrometry (AFS) results of samples containing mixed mercury.

to-use, and instrument-independent method for the on-site detection of mercury pollution in cosmetics.

Declaration of competing interest

The authors declare that they have no known competing financial interests or personal relationships that could have appeared to influence the work reported in this paper.

CRediT authorship contribution statement

Mingzhang Guo: Methodology, Investigation, Resources, Writing - original draft. **Jili Wang:** Methodology, Investigation, Resources. **Ruoxi Du:** Formal analysis. **Yanger Liu:** Data curation. **Jiani Chi:** Visualization. **Xiaoyun He:** Supervision, Conceptualization. **Kunlun Huang:** Project administration, Supervision. **Yunbo Luo:** Project administration, Writing - review & editing. **Wentao Xu:** Conceptualization,

Funding acquisition, Writing - review & editing.

Acknowledgements

This work has been financially supported by the "National GMO Cultivation Major Project of New Varieties" (2018ZX08011-02B) from Ministry of Agriculture and Rural Affairs of the People's Republic of China.

Appendix A. Supplementary data

Supplementary data to this article can be found online at https://doi.org/10.1016/j.bios.2019.111899.

References

Anders, S., Huber, W., 2010. Differential expression analysis for sequence count data. Genome Biol. 11, R106.

Anders, S., Pyl, P.T., Huber, W., 2015. Htseq-a python framework to work with high-throughput sequencing data. Bioinformatics 31 (2), 166–169.

Bjorklund, G., Dadar, M., Mutter, J., Aaseth, J., 2017. The toxicology of mercury: current research and emerging trends. Environ. Res. 159, 545–554.

Cai, S., Shen, Y., Zou, Y., Sun, P., Wei, W., Zhao, J., Zhang, C., 2018. Engineering highly sensitive whole-cell mercury biosensors based on positive feedback loops from quorum-sensing systems. Analyst 143, 1–5.

Chan, T.Y.K., 2011. Inorganic mercury poisoning associated with skin-lightning cosmetic products. Clin. Toxicol. 49 (10), 886–891.

Chen, L.H., Yang, S.L., Chung, K.R., 2014. Resistance to oxidative stress via regulating siderophore-mediated iron acquisition by the citrus fungal pathogen alternaria alternata. Microbiology 160 (5), 970–979.

Cheng, N., Zhu, P., Xu, Y., Huang, K., Luo, Y., Yang, Z., Xu, W., 2016. High-sensitivity assay for Hg (II) and Ag (I) ion detection: a new class of droplet digital PCR logic gates for an intelligent DNA calculator. Biosens. Bioelectron. 84, 1–6, 2016.

Du, R., Guo, M., He, X., Huang, K., Luo, Y., Xu, W., 2019. Feedback regulation mode of gene circuits directly affects the detection range and sensitivity of lead and mercury microbial biosensors. Anal. Chim. Acta 1084, 85–92, 2019.

Feng, Y., Shao, X., Huang, K., Tian, J., Mei, X., Luo, Y., Xu, W., 2018. Mercury nanoladders: a new method for DNA amplification, signal identification and their application in the detection of Hg (II) ions. Chem. Commun. 54 (58), 8036–8039.

Gonzalez-Raymat, H., Liu, G., Liriano, C., Li, Y., Yin, Y., Shi, J., Jiang, G., Cai, Y., 2017. Elemental mercury: its unique properties affect its behavior and fate in the environment. Environ. Pollut. 229, 69–86.

Grandjean, P., Satoh, H., Murata, K., Eto, K., 2010. Adverse effects of methylmercury: environmental health research implications. Environ. Health Perspect. 118 (8), 1137–1145.

Guo, M., Du, R., Xie, Z., He, X., Huang, K., Luo, Y., Xu, W., 2019. Using the promoters of MerR family proteins as "rheostats" to engineer whole-cell heavy metal biosensors with adjustable sensitivity. J. Biol. Eng. 13 (1), 1–9.

Guo, Z., Duan, J., Yang, F., Li, M., Hao, T., Wang, S., Wei, D., 2012. A test strip platform based on dna-functionalized gold nanoparticles for on-site detection of mercury (ii) ions. Talanta 93 (2), 49–54.

Harkins, M., Porter, A.J.R., Paton, G.I., 2004. The role of host organism, transcriptional switches and reporter mechanisms in the performance of hg-induced biosensors. J. Appl. Microbiol. 97 (6), 1192–1200.

Hondroulis, E., Liu, C., Li, C.Z., 2010. Whole cell based electrical impedance sensing approach for a rapid nanotoxicity assay. Nanotechnology 21 (31), 315103.

Langmead, B., Trapnell, C., Pop, M., Salzberg, S.L., 2009. Ultrafast and memory-efficient alignment of short dna sequences to the human genome. Genome Biol. 10 (3), R25.

Leopold, K., Foulkes, M., Worsfold, P., 2010. Methods for the determination and speciation of mercury in natural waters—a review. Anal. Chim. Acta 663 (2), 127–138.

Li, C.Z., Vandenberg, K., Prabhulkar, S., Zhu, X., Schneper, L., Methee, K., Rosser, C.J., Almeide, E., 2011. Paper based point-of-care testing disc for multiplex whole cell bacteria analysis. Biosens. Bioelectron. 26 (11), 4342–4348.

Lori, C., Jeff, F., Tracy, B., Nancy, M.G., 2015. Mercury toxicity and contamination of households from the use of skin creams adulterated with mercurous chloride (calomel). Int. J. Environ. Res. Public Health 12 (9), 10943–10954.

Mahbub, K., Krishnan, K., Naidu, R., Megharaj, M., 2017. Development of a whole cell biosensor for the detection of inorganic mercury. Environ. Technol. Innovat. 8, 64–70.

Mao, X., Cai, T., Olyarchuk, J.G., Wei, L., 2005. Automated genome annotation and pathway identification using the kegg orthology (ko) as a controlled vocabulary. Bioinformatics 21 (19), 3787–3793.

Özkaya, E., Mirzoyeva, L., Ötkür, B., 2010. Mercury-induced systemic allergic dermatitis caused by 'white precipitate' in a skin lightning cream. Contact Dermatitis 60 (1), 61–63.

Patel-Sorrentino, N., Benaim, J.Y., Cossa, D., Lucas, Y., 2011. Synthesis of hydrochloric acid solution for total mercury determination in natural waters. Anal. Bioanal. Chem. 399 (3), 1389–1392.

Pelclova, D., Lukas, E., Urban, P., Preiss, J., Rysava, R., Lebenhart, P., Okrouhlik, B., Fenclova, Z., Lebedova, P., Okrouhlik, B., Fenclova, Z., Lebedova, J., Stejskalova, A., Ridzon, P., 2002. Mercury intoxication from skin ointment containing mercuric ammonium chloride. Int. Arch. Occup. Environ. Health 75 (1 Suppl.), 54–59.

Shao, X., Feng, Y., Zhu, L., Zhang, Y., Luo, Y., Mei, X., Xu, W., 2019. Three dimensional DNA nanotracks: a novel method for ultrasensitive and visible mercury (II) detection. Sens. Actuators B Chem. 303 (2020):126988.

Spiegel, S.J., 2017. New mercury pollution threats: a global health caution. Lancet 390 (10091), 226.

Stocker, J., Balluch, D., Gsell, M., Harms, H., Feliciano, J., Daunert, S., Malik, K.A., Van Der Meer, J.R., 2003. Development of a set of simple bacterial biosensors for quantitative and rapid measurements of arsenite and arsenate in potable water. Environ. Sci. Technol. 37 (20), 4743–4750.

Struss, A., Pasini, P., Ensor, C.M., Raut, N., Daunert, S., 2010. Paper strip whole cell biosensors: a portable test for the semiquantitative detection of bacterial quorum signaling molecules. Anal. Chem. 82 (11), 4457–4463.

Xiao, X., Zhu, L., He, W., Luo, Y., Xu, W., 2019. Functional nucleic acids tailoring and its application. Trends Anal. Chem. 118, 138–157, 2019.

Xu, W., Tian, J., Luo, Y., Zhu, L., Huang, K., 2017. A rapid and visual turn-off sensor for detecting copper (II) ion based on DNAzyme coupled with HCR-based HRP concatemers. Sci. Rep. 7 https://doi.org/10.1038/srep43362, 43362.

Zhu, L., Miao, M., Shao, X., Du, Z., Huang, K., Luo, Y., Xu, W., 2019. A universal electrochemical biosensor using nick-HCR nanostructure as molecular gate of nanochannel for detecting Chromium (III) ions and microRNA. Anal. Chem. https://doi.org/10.1021/acs.analchem.9b03489.

Zhu, P., Tian, W., Cheng, N., Huang, K., Luo, Y., Xu, W., 2016. Ultra-sensitive "turn-on" detection method for Hg2+ based on mispairing biosensor and emulsion PCR. Talanta 155, 168–174, 2016.